ELSEVIER

Journal of Alloys and Compounds 408–412 (2006) 1084–1089

Journal of ALLOYS AND COMPOUNDS

www.elsevier.com/locate/jallcom

Oxygen permeation and methane reforming properties of ceria-based composite membranes

H. Takamura [a,b,*], T. Kobayashi [a], T. Kasahara [a], A. Kamegawa [a], M. Okada [a]

[a] *Department of Materials Science, Graduate School of Engineering, Tohoku University, Aoba-yama 6-6-02, Sendai 980-8579, Japan*
[b] *CREST, Japan Science and Technology Agency, Japan*

Received 30 July 2004; received in revised form 15 December 2004; accepted 15 December 2004
Available online 1 June 2005

Abstract

The preparation and oxygen permeation properties of novel composites of $Ce_{0.9}Sm_{0.1}O_{1.95}$–x vol% $Mn_{(1.5-0.5y)}Co_{(1+0.5y)}Ni_{0.5}O_4$ (CSO–xMCNO; $5 \leq x \leq 25$; $0 \leq y \leq 1.0$) have been investigated. The composites were prepared by the Pechini process to obtain fine microstructures. The composites fired at 1300 °C for 2 h were found to consist of $Ce_{0.9}Sm_{0.1}O_{1.95}$ and two different spinel-type oxides. The oxygen flux density of 0.3 mm-thick CSO–15MCNO with $y = 1.0$ was found to be 1.1 and 7.5 μmol cm^{-2} s^{-1} at 1000 °C under He (20 sccm)/air and Ar–10%CH_4 (100 scm)/air gradients, respectively. CSO–25MCNO with a larger amount of spinel-type phases exhibited a high oxygen flux density of 6.2 μmol cm^{-2} s^{-1} and CO selectivity of 72% at 1000 °C without a conventional reforming catalyst. In addition, $Ce_{0.9}Sm_{0.1}O_{1.95}$–15 vol% $MnFe_2O_4$ (CSO–15MFO) membranes were prepared by means of tape-casting technique. As a result of the optimization of slurry composition, a crack-free dense membrane with dimensions of 5 cm × 5 cm was successfully prepared after sintering at 1300 °C for 2 h. For the tape-cast 133 μm-thick membrane, an oxygen flux density of 9.5 μmol cm^{-2} s^{-1} was attained at 1000 °C. Laminated membranes has been also successfully prepared.

Keywords: Electrode materials; Powder metallurgy; Electrochemical reaction; Syngas production; Hydrogen production

1. Introduction

Oxygen permeation membranes based on mixed oxide-ion and electronic conductors have been attracting much attention of many researchers, in view of their promising applications, such as production of pure oxygen from air and hydrogen from methane [1,2]. To date, a number of oxygen permeable materials based on mixed conductors have been developed. Among them, perovskite-type oxides in La–Sr–Co–Fe and La–Sr–Ga–Fe systems are well known to exhibit a high oxygen flux density, jO_2, at elevated temperatures. For example, $La_{0.7}Sr_{0.3}Ga_{0.6}Fe_{0.4}O_{3-\delta}$ exhibits a high oxygen flux density of approximately 8.2 μmol cm^{-2} s^{-1} at 1000 °C under the reaction of partial oxidation of methane [3].

In addition to those, dual-phase-type mixed conductors comprising of ionic and electronic conductive phases have been developed. For example, composites consisting of Gd-doped CeO_2 (CGO) as an ion-conductive matrix and Sr-doped $LaMnO_3$ (LSM) or Ca-doped $GdCoO_3$ (GCC) responsible for electronic conduction have been reported to exhibit a superior mixed conductivity and the resulting high oxygen flux density [4,5]. As a novel member of composite-type mixed conductors, recently, CGO–15 vol% $MnFe_2O_4$ (MFO) was found to show a high jO_2 of 7 μmol cm^{-2} s^{-1} at 1000 °C under the same methane conversion reaction [6]. For this composite consisting of acceptor-doped ceria and spinel-type ferrites, the optimization of oxygen flux density with respect to the acceptor elements in ceria phase and the volume fraction of spinel-type phase has been conducted; as a result, $Ce_{0.9}Sm_{0.1}O_{1.95}$–15 vol% $MnFe_2O_4$ (CSO–MFO) with a high oxygen flux density has been developed [7].

* Corresponding author. Tel.: +81 22 795 7335; fax: +81 22 795 7335.
E-mail address: takamura@material.tohoku.ac.jp (H. Takamura).

0925-8388/$ – see front matter © 2005 Elsevier B.V. All rights reserved.
doi:10.1016/j.jallcom.2004.12.139

To further improve the oxygen permeation properties, in this study, a novel spinel-type oxide of $Mn_{(1.5-0.5y)}Co_{(1+0.5y)}Ni_{0.5}O_4$ (MCNO; $0 \le y \le 1$) was adopted as an electronic conductive phase instead of MFO. Compared to MFO that shows an electronic conductivity of $8\,S\,cm^{-1}$ at 900 °C, MCNO reportedly shows a higher conductivity of $15\,S\,cm^{-1}$ at 300 °C [8]. Based on its high electronic conductivity, the new composites comprising of CSO and MCNO are expected to show high oxygen flux density as well as CSO–15MFO. Furthermore, since MCNO contains Ni as a constituent cation, CSO–MCNO composites themselves may work as a reforming catalyst. Thus, the first purpose of this study is to prepare the composite membranes consisting of CSO and MCNO, and then evaluates their oxygen permeation and methane reforming properties.

In addition to exploring novel oxygen permeable membranes, from application viewpoints, such as hydrogen production from methane, it is important to develop fabrication techniques of large-size and thin membranes. Therefore, the second purpose of this study is to fabricate large-size and thin CSO–MFO membranes by means of doctor-blade-type tape-casting technique.

2. Experimental

For composite-type materials, it is essential to obtain fine microstructures to achieve high mixed conductivity and the resultant oxygen flux density. Therefore, the composites of $Ce_{0.9}Sm_{0.1}O_{1.95}$–x vol% $Mn_{(1.5-0.5y)}Co_{(1+0.5y)}Ni_{0.5}O_4$ ($5 \le x \le 25$; $0 \le y \le 1$) were prepared by the Pechini process [9–11]. Raw materials used were nitrates and hydroxides serving as metal sources, and citric acid and ethylene glycol serving as chelating agents. After polymerizing, carbonizing and calcination at 700 °C, oxide powders were finally sintered at 1300 °C for 2 h. Reforming catalysts were also prepared by the same technique. The catalysts used were 10 mass% Ni supported on $Ce_{0.9}Pr_{0.1}O_{2-\delta}$ [7].

For tape-casting, the oxide powders of $Ce_{0.9}Sm_{0.1}O_{1.95}$–15 vol% $MnFe_2O_4$ were prepared by the Pechini process as well. The resultant powders were mixed with solvents (2-propanol), dispersants (terpineol [12] or phosphate ester [13]), binders (poly-vinyl-butyral (PVB)) and plasticizers (dibutyl phthalate (DBP) and polyethylene glycol (PEG)); the amount of additives was optimized to give appropriate viscosity. The viscosity of slurries was evaluated by cone-plate-type viscometer prior to tape-casting. The slurry was tape-cast by using doctor-blade-type apparatus. After tape-casting, green sheets were sintered at 1300 °C for 2–5 h.

The set-up for oxygen permeation and methane conversion tests was described elsewhere [6]. Diamond-polished (both sides) samples of approximately ϕ8 mm and approximately 0.3 mm in thickness were sealed with gold and borosilicate glass rings. The samples were then subjected to various pO_2 gradients between air and either He, Ar–5%H_2 or Ar–10%CH_4 within the temperature range of 800–1000 °C. Sweep gases were fed at a rate of 20–270 [STP]$cm^3\,min^{-1}$ (sccm). Gas concentration was determined by use of a gas chromatograph and a mass spectrometer. For methane conversion tests, Ar–5%H_2 gas was swept to activate the catalyst prior to Ar–10%CH_4 gas flow. For the methane conversion tests, oxygen flux densities were calculated from concentrations of CO and CO_2, and CO selectivity was calculated as follows:

$$\text{CO selectivity}\,(\%) = \frac{[\text{CO}]}{([\text{CO}] + [\text{CO}_2])} \times 100 \quad (1)$$

where [CO] and [CO_2] denote concentrations of the respective gases.

3. Results and discussion

3.1. $Ce_{0.9}Sm_{0.1}O_{1.95}$–x vol% $Mn_{(1.5-0.5y)}Co_{(1+0.5y)}Ni_{0.5}O_4$ (CSO–MCNO) composites

First of all, phase identification was performed for $Ce_{0.9}Sm_{0.1}O_{1.95}$–15 vol% $Mn_{(1.5-0.5y)}Co_{(1+0.5y)}Ni_{0.5}O_4$ (CSO–15MCNO), where $0 \le y \le 1$. From XRD analyses as shown in Fig. 1, all the samples fired at 1300 °C for 2 h were found to consist of ceria and spinel-type phases as expected; however, compared to conventional CSO–15MFO composites, reflections assigned to the spinel-type phase seem to be broad and weak. This may suggests the disproportionation or decomposition of the spinel-type phase. Even though Abe et al. reported that MCNO can be obtained as a single phase,

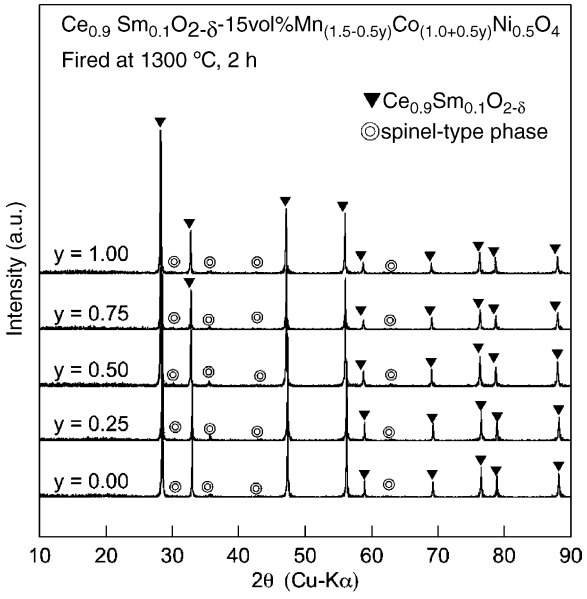

Fig. 1. The X-ray diffraction patterns of $Ce_{0.9}Sm_{0.1}O_{1.95}$–15 vol% $Mn_{(1.5-0.5y)}Co_{(1+0.5y)}Ni_{0.5}O_4$ (CSO–15MCNO; $0 \le y \le 1$) fired at 1300 °C for 2 h.

and shows the following cation distribution [8]:

$$(Co^{2+}_{(0.58+0.33x)}Mn^{2+}_{(0.42-0.33x)})[Ni^{2+}_{0.5}Co^{3+}_{(0.42+0.17x)} \times Mn^{3+}_{(0.58-0.17x)}Mn^{4+}_{0.5}O^{2-}_4 \quad (2)$$

a few spinel phases with different chemical composition may be formed in the CSO–15MCNO composites. Therefore, a microstructural analysis was performed by using SEM–EDS. Fig. 2 shows the back-scattering-electron image of the CSO–15MCNO ($y = 1$) composite fired at 1300 °C for 2 h. As can be seen, a well sintered and dispersed composite was obtained under this sintering condition; however, further increase in firing temperature caused decrease in a relative density down to less than 90%, presumably due to a so-called "swelling effect". With respect to compositional analysis, three phases, i.e. white, gray and black contrasts, were found to exist. The white phase was identified as a $Ce_{0.9}Sm_{0.1}O_{1.95}$ matrix phase. Its grain size was approximately 2 μm, in which the incorporation of a few percent of Mn and Co was confirmed. Regarding the spinel-type phases, the cation ratio (Mn:Co:Ni) of phases with black and gray contrasts was estimated as 1:1:0.2 and 0:0.5:0.25, respectively. Thus, the CSO–15MCNO composite was found to consist of $Ce_{0.9}Sm_{0.1}O_{1.95}$, Mn–Co–Ni and Ni–Co-based spinel-type phases. The two spinel-type phases were also found to exist in the samples with different values of x (volume fraction) and y (Co content).

The oxygen flux density of CSO–15MCNO was evaluated as a function of Co content of y as shown in Fig. 3. The oxygen flux density was measured within the temperature range of 800 to 1000 °C under He (20 sccm)/air or Ar–10%CH_4 (100 sccm)/air gradients. The membrane thickness was fixed to be approximately 0.3 mm. For He/air gradient (Fig. 3(a)), an oxygen flux density, jO_2, increased with increasing Co content of y; the sample with $y = 1$ showed a jO_2 of 1.1 μmol cm^{-2} s^{-1}, which is larger by a factor of approximately two than that for the case of $y = 0$. Under the Ar–10%CH_4/air gradient (Fig. 3(b)), the CSO–15MCNO composites with $y = 1.0$ showed a high jO_2 of 3.0 and 7.5 μmol cm^{-2} s^{-1} at 800 and 1000 °C, respectively. These jO_2 values for the CSO–15MCNO composite are almost comparable to those for CSO–15MFO previously reported (2–3 and 6–7 μmol cm^{-2} s^{-1} at 800 and 1000 °C, respectively, at a flow rate of 100 sccm) [7]. Even though the role of two spinel-type phases, i.e. Mn–Co–Ni and Ni–Co-based phases, has to be further investigated, judging from their high jO_2 values, the novel CSO–MCNO composites may be used for methane conversion applications.

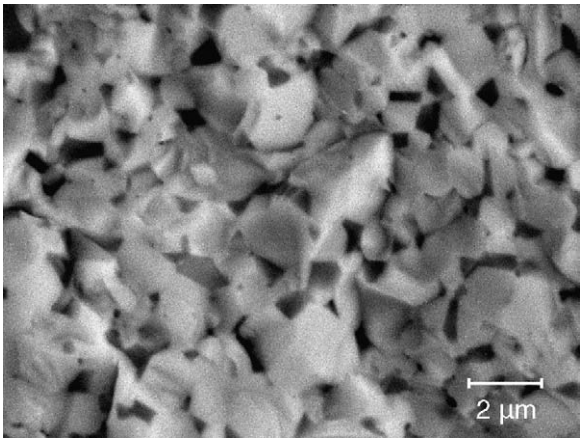

Fig. 2. Back-scattering electron micrograph of $Ce_{0.9}Sm_{0.1}O_{1.95}$–15 vol% $MnCo_{1.5}Ni_{0.5}O_4$ (CSO–15MCNO) fired at 1300 °C for 2 h.

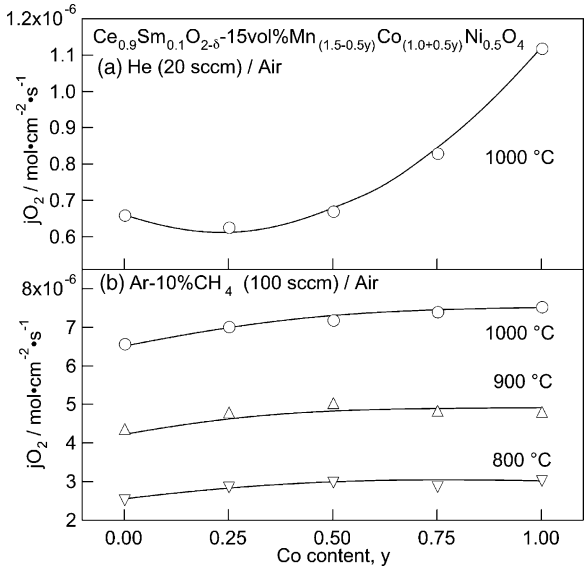

Fig. 3. The oxygen flux density of $Ce_{0.9}Sm_{0.1}O_{1.95}$–15 vol% $Mn_{(1.5-0.5y)}Co_{(1+0.5y)}Ni_{0.5}O_4$ (CSO–15MCNO; $0 \le y \le 1$) under (a) He (20 sccm)/air and (b) Ar–10%CH_4 (100 sccm)/air gradients.

The stability of oxygen flux density with respect to elapsed time is also one of the important characteristics for oxygen permeable membranes, since the membranes subjected to large pO_2 gradients between reformed gas and air may cause phase decomposition. Fig. 4 shows the time dependence of oxygen flux density for the composites with 15 and 25 vol% MCNO ($y = 1$) at 1000 °C under Ar–10%CH_4 (100 sccm)/air gradient. Both composites showed a certain level of degradation of jO_2 until 5 h. After that, however, jO_2 appears to be almost constant. Even though the duration of measurements is limited to 24 h, these CSO–MCNO composites seem to have enough chemical stability under methane conversion environments.

As another aspect, the catalytic activity of CSO–MCNO composites was evaluated. As described in experimental details, the 10 mass% Ni catalyst supported on $Ce_{0.9}Pr_{0.1}O_{2-\delta}$ have been usually used to promote the reaction of partial oxidation of methane for the oxygen flux density measurements under Ar–10%CH_4/air gradients. Since CSO–MCNO composites contain Ni as a constituent cation these membranes themselves may exhibit a certain level of catalytic activity. Therefore, the oxygen permeation and methane reforming properties of the CSO–MCNO composites were measured

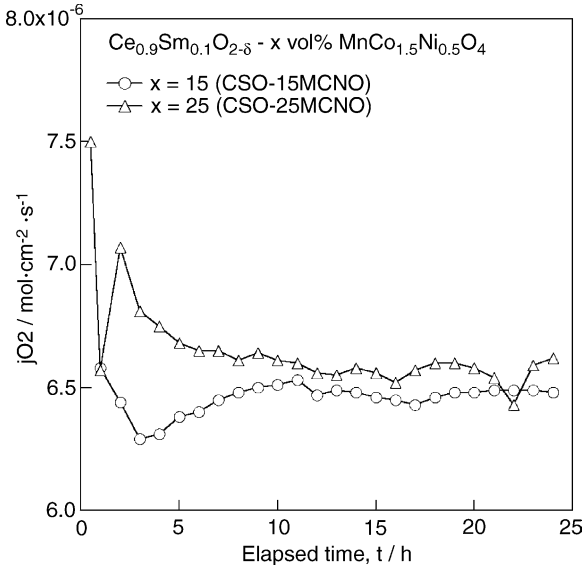

Fig. 4. The oxygen flux density of $Ce_{0.9}Sm_{0.1}O_{1.95}$–x vol% $MnCo_{1.5}Ni_{0.5}O_4$ (CSO–15MCNO), where $x = 15$ or 25, at 1000 °C under Ar–10%CH_4 (100 sccm)/air gradient.

without putting the 10 mass% Ni–$Ce_{0.9}Pr_{0.1}O_{2-\delta}$ catalyst on the surface of composite membranes. Table 1 summarizes jO_2 and the CO selectivity of CSO–MCNO ($y = 1.0$) and CSO–MFO composites. Compared to CSO–15MCNO with the reforming catalyst (Fig. 3(b)), all the samples without the reforming catalyst showed lower oxygen flux density. However, CSO–25MCNO without the reforming catalyst exhibited a relatively high jO_2 of 6.2 μmol cm^{-2} s^{-1}, which is comparable to that for CSO–15MFO with reforming catalyst. This relatively high jO_2 may be attributed to the presence of Ni-containing spinel-type phases. Even though CO selectivity (72%) must be further improved, the CSO–25MCNO composite itself appears to have a catalytic activity with respect to the partial oxidation of methane.

From these observations, the characteristics of novel CSO–15MCNO composites can be summarized as follows: (1) the CSO–MCNO composites consisted of $Ce_{0.9}Sm_{0.1}O_{1.95}$ and two different spinel-type oxides; (2) the oxygen flux density of CSO–MCNO was comparable to that for the CSO–MFO composites and (3) CSO–25MCNO exhibited a high jO_2 of 6.2 μmol cm^{-2} s^{-1} at 1000 °C without a reforming catalyst.

Table 1
The oxygen flux density and CO selectivity of CSO–MCNO and CSO–MFO composites without a reforming catalyst

Composites	Thickness (mm)	jO_2 (μmol^{-2} s^{-1})	CO selectivity (%)
CSO–5MCNO	0.34	3.2	56
CSO–15MCNO	0.25	3.5	61
CSO–25MCNO	0.31	6.3	72
CSO–15MfO	0.26	2.7	60

The data were taken at 1000 CircC under Ar–10%CH_4 (270 sccm).

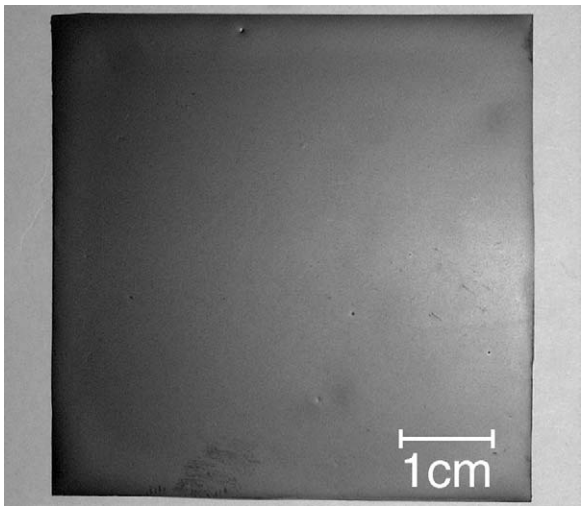

Fig. 5. The tape-cast CSO–15MFO membrane after sintering at 1300 °C for 2 h.

3.2. *Tape-casting of $Ce_{0.9}Sm_{0.1}O_{1.95}$–15 vol% $MnFe_2O_4$ (CSO–15MFO) composite membranes*

Since oxygen permeable materials mentioned above are supposed to be used as membrane applications, it is important to develop fabrication techniques of membranes. In this study, tape-casting, especially, the doctor-blade-type was employed. Prior to tape-casting, it is essential to optimize the amount of slurry additives, such as binder and plasticizer agents. In general, the strength and plasticity of ceramics green sheets depend on the amount of binders and plasticizers, respectively. On the other hand, the excess addition can be a source of the reduction of sintering density, which may cause mechanical N_2-leakages for sintered membranes. As a result of trial and error manner optimization, the composition of ceramics slurry was decided as follows: oxide powders (68.7 mass%), solvent (2-propanol 19.5 mass%), binder (PVB 2.5 mass%), dispersant (terpineol 1.9 mass%) and plasticizer (DBP 5.1 mass% and PEG 2.3 mass%), respectively. In the case of use of phosphate esters as dispersant agents, smooth and stable slurries were obtained [13]; however, residual phosphate compounds appeared to degrade the oxygen flux density. Thus, only terpineol was used as a dispersant agent [12]. The viscosity of slurries was adjusted to be 1000–2000 mPa s by controlling the evaporation of solvent during a vacuum defoaming process. For CSO–15MFO, a crack-free dense membrane with dimensions of 5 cm × 5 cm and 140 μm in thickness was successfully prepared after sintering at 1300 °C for 2 h as shown in Fig. 5. Phases present in sintered ceramics membranes were then analyzed by means of XRD. As a result, the CSO–15MFO membrane after sintering was found to consist of (Ce, Sm)O_2 and $MnFe_2O_4$ phases. These phases present were identical with the bulk material.

Fig. 6 shows Arrhenius-type plots of oxygen flux density and CO selectivity of the tape-cast CSO–15MFO

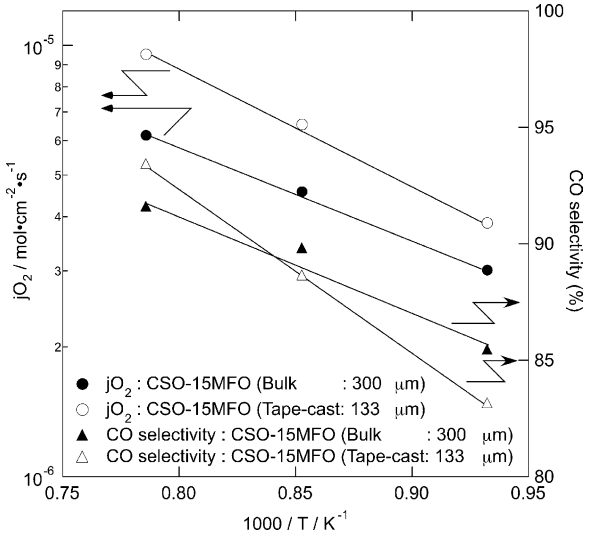

Fig. 6. Arrhenius-type plots of oxygen flux density and CO selectivity of CSO–15MFO membranes.

membrane with a thickness of 133 μm. The oxygen flux density was measured under Ar–10%CH_4 (100 sccm)/air gradients. As a reference, jO_2 for the bulk specimen with same composition but approximately doubled thickness was also plotted. As a result of decrease in membrane thickness, the oxygen flux density of CSO–15MFO was enhanced up to 9.5 μmol cm^{-2} s^{-1} at 1000 °C. Even at 800 °C, the tape-cast CSO–15MFO membrane showed a high jO_2 of 3.9 μmol cm^{-2} s^{-1}. Based on the jO_2 values for CSO–15MFO, to produce H_2 for 1 kW-PEFC, a membrane area size of approximately 200 cm^2 is required at 1000 °C. These area sizes can be achieved by using eight sheets of 5 cm × 5 cm-size membranes shown in Fig. 5. For CSO–15MFO, which showed the highest jO_2 of 9.5 μmol cm^{-2} s^{-1} at 1000 °C, the corresponding CO selectivity was 93% under a methane conversion rate of 22%.

With respect to jO_2 obtained for the tape-cast membrane at 1000 °C, note that the value was enhanced only 50% compared to those for the bulk specimen, even though the membrane thickness was reduced by a factor of about 1/2. This implies that the oxygen permeation flux was limited by surface exchange kinetics rather than ambipolar diffusion process in ceramics. If this is the case, the Wagner's equation can be modified by including a characteristic thickness of L_c as follows [14]:

$$jO_2 = \gamma \frac{RT}{16F^2L} \int_{\ln p(O_2)'}^{\ln p(O_2)''} \frac{\sigma_i \sigma_{el}}{\sigma_i \sigma_{el}} \, d \ln p(O_2) \quad (3)$$

where

$$\gamma = \frac{1}{1 + 2(L_c/L)} \quad (4)$$

The term of γ works as a reduction factor for theoretical jO_2; jO_2 can be reduced by a factor of 1/3 in the case of $L = L_c$. In our previous work, jO_2 for $Ce_{0.8}Gd_{0.2}O_{2-\delta}$–15 vol% $MnFe_2O_4$ (CGO–15MFO) was evaluated as a function of the membrane thickness [7]. From a fitting analysis, L_c for CGO–15MFO under Ar–5%H_2/air gradients was estimated to be approximately 500 μm. Thus, it would not be surprising to find the limitation of jO_2 due to surface exchange kinetics for CSO–15MFO in the membrane thickness range of 100–300 μm.

To further increase the oxygen flux density of jO_2, laminated membrane structures were examined. From our previous work, it is found that higher jO_2 can be obtained in the case of use of $CoFe_2O_4$ (CFO) instead of MFO as an electronic conductive phase; however, ceria-based composites with CFO are not chemically stable enough under methane conversion atmosphere [6]. Based on these observations, laminated membrane structures, in which CSO–30CFO layers were laminated on CSO–15MFO layers were fabricated. Prior to lamination process, CSO–15MFO and CSO–30CFO green sheets with a thickness of 30–40 μm were prepared by the same tape-casting technique. By using uniaxial die-press, these thin green sheets were laminated in the manner of CSO–15MFO × (6 − N) + CSO–30CFO × N to be 210 ± 30 μm as total membrane thickness.

Fig. 7 show SEM cross sectional images of laminated membranes of CSO–15MFO × (6 − N) sheets/CSO–30CFO × N sheets, where N = 3, 4 and 5, after sintering at 1300 °C for 5 h. The laminated membranes were successfully sintered without showing any cracks and edge curl, since their thermal expansion coefficients are almost identical (≈1.3×10^{-5} K as an average value between room temperature and 1000 °C). The interface between CSO–15MFO and CSO–30CFO can be seen as different contrast. From the magnified image (Fig. 7(d)), the adhesion between CSO–15MFO and CSO–30CFO layers appears to be good. For methane conversion tests, the CSO–30CFO layer was exposed to air-feed side. Fig. 8 shows oxygen flux density of CSO–15MFO/CSO–30CFO laminated membranes at 1000 °C as a function of the number of

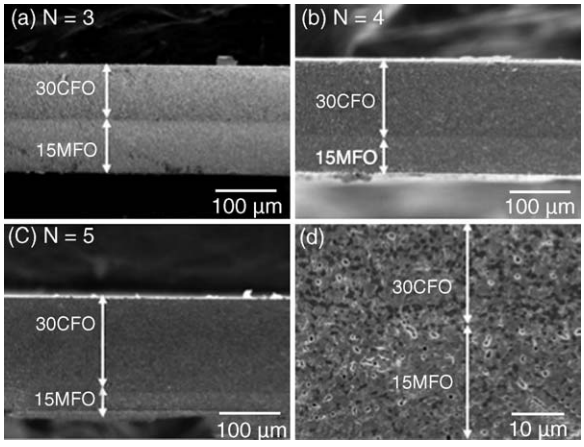

Fig. 7. SEM images of cross-section of laminated membranes after sintering at 1300 °C for 5 h. CSO–15MFO and CSO–30CFO were laminated in the manner of CSO–15MFO × (6 − N) + CSO–30CFO × N. (a) N = 3, (b) N = 4 and (c) N = 5. The magnified image of interface between CSO–15MFO and CSO–30CFO in (a) were shown in (d).

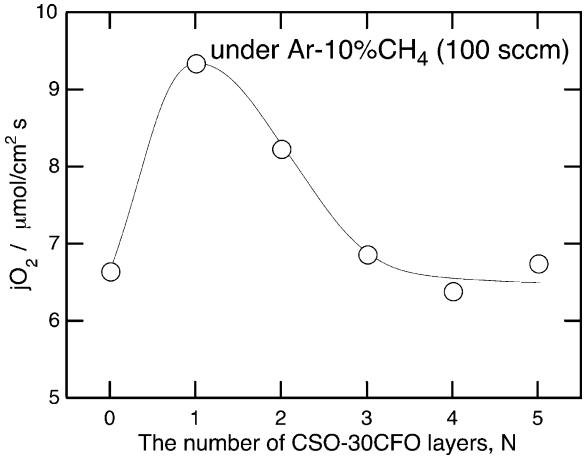

Fig. 8. The oxygen flux density of laminated membranes as a function of the number of CSO–30CFO layers.

CSO–30CFO layers. The membrane thickness was in the range of 180–240 μm. As expected, in the case of $N = 1$, i.e. CSO–15MFO × 5 + CSO–30CFO × jO_2 increased by a factor of 40% compared to the CSO–15MFO × 6 ($N = 0$) membrane. This enhancement may suggest that the lamination of oxygen permeable membranes with high jO_2 and high chemical stability is effective to improve the oxygen flux density. However, further increase in the number of CSO–30CFO reduced jO_2, presumably due to the partial decomposition of CFO phase. In fact, in the case of $N = 4$ or higher, the laminated membranes were cracked during the methane conversion tests.

4. Conclusions

The preparation and oxygen permeation properties of novel composite-type oxygen permeable ceramics of $Ce_{0.9}Sm_{0.1}O_{1.95}$–x vol% $Mn_{(1.5-0.5y)}Co_{(1+0.5y)}Ni_{0.5}O_4$ (CSO–xMCNO; $5 \leq x \leq 25$; $0 \leq y \leq 1$) have been firstly investigated. The composites fired at 1300 °C for 2 h were found to consist of $Ce_{0.9}Sm_{0.1}O_{1.95}$ and two different spinel-type oxides. The oxygen flux density of 0.3 mm-thick CSO–15MCNO with $y = 1.0$ was found to be 1.1 and 7.5 μmol cm^{-2} s^{-1} at 1000 °C under He (20 sccm)/air and Ar–10%CH_4 (100 sccm)/air gradients, respectively. In addition, CSO–25MCNO exhibited a high jO_2 of 6.2 μmol cm^{-2} s^{-1} and CO selectivity of 72% at 1000 °C without a reforming catalyst, presumably due to the presence of Ni in the composites.

Furthermore, the preparation of $Ce_{0.9}Sm_{0.1}O_{1.95}$–15 vol% $MnFe_2O_4$ (CSO–15MFO) membranes by means of tape-casting technique and their oxygen permeation properties have been also investigated. A crack-free dense membrane with dimensions of 5 cm × 5 cm was successfully prepared after sintering at 1300 °C for 2 h. For the 133 μm-thick CSO–15MFO membrane, an oxygen flux density of 9.5 μmol cm^{-2} s^{-1} was attained at 1000 °C. Laminated membranes comprising of CSO–15MFO and CSO–30CFO were also prepared. The laminated membrane with one CSO–30CFO layer showed a higher oxygen flux density by a factor of 40% than that without CSO–30CFO layer.

Acknowledgements

This work has been supported by CREST of Japan Science and Technology Corporation (JST), The Japan Research and Development Center for Metals (JRCM), and Ministry of Education, Science, Sports and Culture, Grant-in-Aid for Young Scientists (B), No. 15760512.

References

[1] Y. Teraoka, H.M. Zhang, S. Furukawa, N. Yamazoe, Chem. Lett. (1985) 1743–1746.
[2] P.N. Dyer, R.E. Richards, S.L. Russek, D.M. Taylor, Solid State Ionics 134 (2000) 21–33.
[3] T. Ishihara, Y. Tsuruta, T. Todaka, H. Nishiguchi, Y. Takita, Solid State Ionics 152 (2002) 709–714.
[4] V.V. Kharton, A.V. Kovalevsky, A.P. Viskup, F.M. Figueiredo, A.A. Yaremchenko, E.N. Naumovich, F.M.B. Marques, J. Eur. Ceram. Soc. 21 (2001) 1763–1767.
[5] U. Nigge, H.D. Wiemhofer, E.W.J. Romer, H.J.M. Bouwmeester, T.R. Schulte, Solid State Ionics 146 (2002) 163–174.
[6] H. Takamura, M. Kawai, K. Okumura, A. Kamegawa, M. Okada, in: P. Knauth, J.-M. Tarascon, E. Traversa, H.L. Tuller (Eds.), Solid State Ionics - 2002: Mat. Res. Soc. Symp. Proc., vol. 756, Materials Research Society, Warrendale, 2003, pp. EE8.11.11–EE.8.11.16.
[7] H. Takamura, K. Okumura, Y. Koshino, A. Kamegawa, M. Okada, J. Electroceram. 13 (2004) 613–618.
[8] Y. Abe, T. Meguro, T. Yokoyama, T. Morita, J. Tatami, K. Komeya, J. Ceram. Process. Res. 4 (2003) 140–144.
[9] M.P. Pechini, US Patent #3,330,697 (1967).
[10] H. Takamura, H.L. Tuller, Solid State Ionics 134 (2000) 67–73.
[11] H. Takamura, K. Enomoto, A. Kamegawa, M. Okada, Solid State Ionics 154 (2002) 581–588.
[12] A.K. Maiti, B. Rajender, Mater. Sci. Eng. A 333 (2002) 35–40.
[13] M.W. Murphy, T.R. Armstrong, P.A. Smith, J. Am. Ceram. Soc. 80 (1997) 165–170.
[14] H.J.M. Bouwmeester, H. Kruidhof, A.J. Burggraaf, Solid State Ionics 72 (1994) 185–194.